JOURNAL OF GUIDANCE, CONTROL, AND DYNAMICS
Vol. 19, No. 6, November–December 1996

Sensor Placement for Time-Domain Modal Parameter Estimation

Chinchao Liu* and Frederick A. Tasker†
University of Maryland Baltimore County, Baltimore, Maryland 21228-5398

A new method of sensor placement for modal identification is presented. The sensor placement technique utilizes the variance of estimates derived from a perturbation analysis of a time-domain parameter estimation method to determine appropriate locations of sensors. An efficient scheme is developed to implement the backward elimination scheme for sensor placement. The performance of this method is compared with two alternatives: a process of maximizing the determinant of the Fisher information matrix corresponding to the target modal partitions and a process of minimizing the trace of the covariance matrix. The effect of finite element model error on this placement technique is investigated. Numerical examples demonstrate the efficiency and effectiveness of the new approach.

I. Introduction

THE objective of modal parameter estimation is to obtain modal parameters and to quantify the accuracy of such estimates using measures such as bias and variance. These quantities, however, depend on the locations of the sensors, which leads to a problem of optimal placement of sensors. Limitations in the number of sensors, especially for space structures, and the importance of modal parameters in modal refinement and damage detection further necessitate optimal placement of sensors.

Optimal placement of sensors is an experiment design problem. In general, the efficient estimator is often chosen that achieves the minimum covariance of all unbiased estimators. It is known that when this estimator exists, it necessarily has to be a maximum likelihood estimator. To perform sensor location, a scalar measure of the covariance matrix or its inverse, the Fisher information matrix, is optimized. Note, however, that it is very unusual to use a maximum likelihood estimator for general multioutput, multimode modal testing. Because sensor placement is heavily dependent on the choice of the parameter estimation algorithm, the popular time-domain methods for modal parameter estimation are considered. The method developed here for optimization of locations uses variances obtained by the application of a stochastic perturbation approach to the practical time-domain methods. This approach avoids the unrealistic assumption of an efficient estimator in the problem of sensor placement for modal parameter estimation.

Time-domain methods of modal parameter estimation are particularly useful for multichannel data consisting of a large number of modes, some of which may be closely spaced. The first few time-domain methods were introduced in the late 1970s and early 1980s, such as the complex exponential method,[1,2] the Ibrahim time domain,[2,3] and the polyreference method.[4–6] In the mid-1980s, the eigensystem realization algorithm (ERA) was introduced by Juang and Pappa.[7–10] Numerous time-domain methods have been proposed in recent years.[11–15] It can be shown that these methods differ only in the reduced-rank method used to solve a linear system of equations.

Work on sensor placement for parameter identification was done by Qureshi et al.[16] using the determinant of the Fisher information matrix of parameters as a criterion. Yu and Seinfeld[17] and Omatu et al.[18] also address sensor placement for state estimation by minimizing the trace of the steady-state covariance matrix of state estimates. Bayard et al.[19] stated that the sensor placement and input design problems can be decoupled and solved independently for modal parameter estimation. In all of the above cases, an efficient estimator was assumed. Delorenzo[20] developed effectiveness measures for sensors and actuators to maximize the performance of a linear quadratic Gaussian control scheme. This method was based on the backward elimination scheme.[21] Kammer[22–24] formulated an effective independence approach for the ranking of sensors based on their contribution to the determinant of the Fisher information matrix of the estimated modal responses. This method also uses the backward elimination approach. However, it applies to the modal filtering problem. These schemes, with one exception,[18] however, did not directly address modal parameter estimation. However, the method did not employ a practical parameter estimation scheme. This paper develops an efficient scheme for sensor placement, using the backward elimination scheme, for time-domain modal parameter estimation. Because this placement technique is dependent on the finite element method (FEM) of the structure, the issue of how finite element modeling error affects the placement strategies also is explored.

II. Variance of Parameter Estimates

The first step in the optimization of sensor locations is the determination of an appropriate optimization criterion. We use the variance of the estimated modal parameters. The derivation of the variance of modal parameters estimated by time-domain methods was formulated by Hua and Sarkar[25] using a matrix-pencil formulation. Another approach has been presented for the ERA method.[9] The results of the ERA method and the matrix-pencil approach[25] are quite similar for the multioutput problem considered here. The estimated variance is the effect of small stochastic perturbations to the data and therefore is valid for moderate to high signal-to-noise ratios.[26,27] We extend the single input/single output case[25] to the single input/multioutput case and use it as a criterion for ranking of sensors.

A measured response can be written as

$$\hat{y}_r(t) = y_r(t) + \varepsilon_r(t), \qquad r = 1, 2, \ldots, s \tag{1}$$

where

$$y_r(t) = \sum_{i=1}^{m} a_{ri} z_i^t$$

is a free decay or impulse response to a single input; $z_i = \exp(\alpha_i + j\omega_i)$; α_i and ω_i are the decay rates and the damped frequencies, respectively; a_{ri} is the amplitude of the ith mode in the rth output; m and s are the number of modes and outputs, respectively; $\varepsilon_r(t)$ is the noise sequence corresponding to the rth output and

Received Dec. 11, 1994; revision received May 1, 1996; accepted for publication May 10, 1996.

*Research Assistant. Department of Mechanical Engineering. Student Member AIAA.

†Assistant Professor. Department of Mechanical Engineering. Member AIAA.

$E[\varepsilon_l(t_1)\varepsilon_k(t_2)] = \varphi_o^2\delta(l-k)\delta(t_2-t_1)$, where δ is the Kronecker delta function. Let us define the $(h \times 1)$ output vector as

$$\boldsymbol{y}_r(j) = [y_r(j) \quad y_r(j+1) \quad \cdots \quad y_r(j+h-1)]^T \tag{2}$$

The $(h \times k)$ Hankel matrices for the rth output then can be formed as

$$\boldsymbol{H}_0^r = [y_r(0) \quad y_r(1) \quad \cdots \quad y_r(k-1)] \tag{3}$$

$$\boldsymbol{H}_1^r = [y_r(1) \quad y_r(2) \quad \cdots \quad y_r(k)] \tag{4}$$

The matrices can be expressed as

$$\boldsymbol{H}_0^r = \boldsymbol{V}_h \boldsymbol{B}_r \boldsymbol{V}_k^T \tag{5}$$

$$\boldsymbol{H}_1^r = \boldsymbol{V}_h \boldsymbol{Z} \boldsymbol{B}_r \boldsymbol{V}_k^T \tag{6}$$

where $(\cdot)^T$ represents the transpose operation, $\boldsymbol{B}_r$ is a diagonal matrix formed by the rth row of the amplitude matrix, $\boldsymbol{V}_h$ and $\boldsymbol{V}_k$ are Vandermonde matrices and are given by

$$\boldsymbol{V}_h = \begin{bmatrix} z_1^0 & z_1^0 & \cdots & z_m^0 & (z_1^*)^0 & (z_2^*)^0 & \cdots & (z_m^*)^0 \\ z_1^1 & z_2^1 & \cdots & z_m^1 & (z_1^*)^1 & (z_2^*)^1 & \cdots & (z_m^*)^1 \\ \vdots & \vdots & \cdots & \vdots & \vdots & \vdots & \cdots & \vdots \\ z_1^{h-1} & z_2^{h-1} & \cdots & z_m^{h-1} & (z_1^*)^{h-1} & (z_2^*)^{h-1} & \cdots & (z_m^*)^{h-1} \end{bmatrix} \tag{7}$$

$$\boldsymbol{V}_k = \begin{bmatrix} z_1^0 & z_1^0 & \cdots & z_m^0 & (z_1^*)^0 & (z_2^*)^0 & \cdots & (z_m^*)^0 \\ z_1^1 & z_2^1 & \cdots & z_m^1 & (z_1^*)^1 & (z_2^*)^1 & \cdots & (z_m^*)^1 \\ \vdots & \vdots & \cdots & \vdots & \vdots & \vdots & \cdots & \vdots \\ z_1^{k-1} & z_2^{k-1} & \cdots & z_m^{k-1} & (z_1^*)^{k-1} & (z_2^*)^{k-1} & \cdots & (z_m^*)^{k-1} \end{bmatrix} \tag{8}$$

$$\boldsymbol{B}_r = \operatorname{diag}\left(\begin{bmatrix} a_{r1} & a_{r2} & \cdots & a_{rm} & a_{r1}^* & a_{r2}^* & \cdots & a_{rm}^* \end{bmatrix}\right) \tag{9}$$

and

$$\boldsymbol{Z} = \operatorname{diag}\left(\begin{bmatrix} z_1 & z_2 & \cdots & z_m & z_1^* & z_2^* & \cdots & z_m^* \end{bmatrix}\right) \tag{10}$$

where $(\cdot)^*$ represents the complex conjugate operation. Then, the data matrices for a multioutput case are given as

$$\boldsymbol{Y}_0 = \begin{bmatrix} \boldsymbol{H}_0^1 & \boldsymbol{H}_0^2 & \cdots & \boldsymbol{H}_0^s \end{bmatrix} = \boldsymbol{V}_h \boldsymbol{V}_b^T \tag{11}$$

$$\boldsymbol{Y}_1 = \begin{bmatrix} \boldsymbol{H}_1^1 & \boldsymbol{H}_1^2 & \cdots & \boldsymbol{H}_1^s \end{bmatrix} = \boldsymbol{V}_h \boldsymbol{Z} \boldsymbol{V}_b^T \tag{12}$$

where

$$\boldsymbol{V}_b^T = \begin{bmatrix} \boldsymbol{B}_1 \boldsymbol{V}_k^T & \boldsymbol{B}_2 \boldsymbol{V}_k^T & \cdots & \boldsymbol{B}_s \boldsymbol{V}_k^T \end{bmatrix} \tag{13}$$

Derive the system matrix $\boldsymbol{S}$ as

$$\boldsymbol{Y}_1 = \boldsymbol{Y}_0 \boldsymbol{S} \tag{14}$$

Then,

$$\boldsymbol{V}_b^T \boldsymbol{S} = \boldsymbol{Z} \boldsymbol{V}_b^T \tag{15}$$

Because $\boldsymbol{Y}_0$ has rank m, $\boldsymbol{S}$ is usually obtained from Eq. (14) using subspace techniques such as the singular value decomposition. The system matrix $\boldsymbol{S} \in R^{sk \times sk}$ has $(sk - 2m)$ zero eigenvalues and $2m$ nonzero eigenvalues, which have the following relationship:

$$\boldsymbol{p}_i^H \boldsymbol{S} = \boldsymbol{p}_i^H z_i, \qquad \boldsymbol{S}\boldsymbol{q}_i = z_i \boldsymbol{q}_i \tag{16}$$

where $\boldsymbol{P} = [\boldsymbol{p}_1 \ \boldsymbol{p}_2 \ \cdots \ \boldsymbol{p}_m \ \boldsymbol{p}_1^* \ \boldsymbol{p}_2^* \ \cdots \ \boldsymbol{p}_m^*]$ and $\boldsymbol{Q} = [\boldsymbol{q}_1 \ \boldsymbol{q}_2 \ \cdots \ \boldsymbol{q}_m \ \boldsymbol{q}_1^* \ \boldsymbol{q}_2^* \ \cdots \ \boldsymbol{q}_m^*]$ are the left and right eigenvectors of $\boldsymbol{S}$, respectively. Obviously from Eq. (16), the left eigenvectors of $\boldsymbol{S}$ are $\boldsymbol{P}^H = \boldsymbol{V}_b^T$; then the right eigenvectors of $\boldsymbol{S}$ are $\boldsymbol{Q} = (\boldsymbol{V}_b^T)^\dagger$, where $(\cdot)^\dagger$ represents the pseudoinverse operation. That $\boldsymbol{Q} = [\boldsymbol{V}_b^T]^\dagger$ is obtained by using $\boldsymbol{P}^H\boldsymbol{Q} = \boldsymbol{I}$ and by the fact that $\boldsymbol{P}$ and $\boldsymbol{Q}$ span the same subspace.

It is known from perturbation theory that the perturbation in the eigenvalues (z_i) attributable to perturbation in the system matrix $\boldsymbol{S}$ can be written as[26]

$$\delta z_i = \frac{\boldsymbol{p}_i^H \delta(\boldsymbol{S}) \boldsymbol{q}_i}{\boldsymbol{p}_i^H \boldsymbol{q}_i} \tag{17}$$

where δ is the first-order differential operator. With some algebraic manipulation,[25] Eq. (17) can be expressed as

$$\delta z_i = \boldsymbol{p}_i^H \boldsymbol{Y}_0^\dagger (\delta \boldsymbol{Y}_1 - z_i \delta \boldsymbol{Y}_0) \boldsymbol{q}_i \tag{18}$$

Note that $\delta \boldsymbol{Y}_1$ and $\delta \boldsymbol{Y}_0$ consist of noise components only. Also, using Theorem (1.4.1) from Ref. 28, $\boldsymbol{Y}_0^\dagger = [\boldsymbol{V}_b^T]^\dagger \boldsymbol{V}_h^\dagger$,

$$\boldsymbol{p}_i^H \boldsymbol{Y}_0^\dagger = \boldsymbol{p}_i^H \left[\left(\boldsymbol{V}_b^T \right)^\dagger \boldsymbol{V}_h^\dagger \right] = \left(\boldsymbol{V}_h^\dagger \right)_i = \boldsymbol{l}_i \tag{19}$$

where $(\boldsymbol{V}_h^\dagger)_i$ is the ith row of $(\boldsymbol{V}_h^\dagger)$. Then, by expanding Eq. (18) and forming a noise vector, an alternative expression can be derived as

$$\delta z_i = \left(\boldsymbol{V}_h^\dagger \right)_i (\delta \boldsymbol{Y}_1 - z_i \delta \boldsymbol{Y}_0) \boldsymbol{q}_i = \boldsymbol{q}_i^T \boldsymbol{R}_i \varepsilon \tag{20}$$

where $\boldsymbol{R}_i \in C^{sk \times sN}$; $N(= h + k)$ is the length of sampled data of each output:

$$\boldsymbol{R}_i = \begin{bmatrix} \boldsymbol{G}_{i0} & 0 & \cdots & 0 \\ 0 & \boldsymbol{G}_{i0} & \cdots & 0 \\ \vdots & \vdots & \ddots & \vdots \\ 0 & 0 & \cdots & \boldsymbol{G}_{i0} \end{bmatrix} - z_i \begin{bmatrix} \boldsymbol{G}_{i1} & 0 & \cdots & 0 \\ 0 & \boldsymbol{G}_{i1} & \cdots & 0 \\ \vdots & \vdots & \ddots & \vdots \\ 0 & 0 & \cdots & \boldsymbol{G}_{i1} \end{bmatrix} \tag{21}$$

and

$$\boldsymbol{G}_{i0} = \begin{bmatrix} 0 & \boldsymbol{l}_i & 0 & \cdots & 0 \\ 0 & 0 & \boldsymbol{l}_i & \cdots & 0 \\ \vdots & \vdots & \vdots & \ddots & 0 \\ 0 & 0 & 0 & \cdots & \boldsymbol{l}_i \end{bmatrix}$$

$$\boldsymbol{G}_{i1} = \begin{bmatrix} \boldsymbol{l}_i & 0 & \cdots & 0 & 0 \\ 0 & \boldsymbol{l}_i & \cdots & 0 & 0 \\ \vdots & \vdots & \ddots & \vdots & \vdots \\ 0 & 0 & \cdots & \boldsymbol{l}_i & 0 \end{bmatrix} \tag{22}$$

Matrices $\boldsymbol{G}_{i0}$ and $\boldsymbol{G}_{i1}$ are arranged such that $\boldsymbol{l}_i$ in each row is shifted right by one position from the previous row and repeated k times; $\boldsymbol{G}_{i0}$ and $\boldsymbol{G}_{i1} \in C^{k \times N}$. The noise vector $\varepsilon \in C^{sN \times 1}$ is given as

$$\varepsilon = [\varepsilon_1(0) \quad \varepsilon_1(1) \cdots \varepsilon_1(N-1) \cdots \varepsilon_s(0) \quad \varepsilon_s(1) \cdots \varepsilon_s(N-1)]^T \tag{23}$$

where $\varepsilon_i(j)$ is the noise at j time in ith output. Equation (20) implies that δz_i is a random variable because it is a function of the random vector ε. Assume that the variances of noise for all of the outputs are φ_o^2; then, the first-order estimate of the variance of the estimate of z_i is

$$\operatorname{var}(\delta z_i) = \varphi_o^2 \left[\boldsymbol{q}_i^T \boldsymbol{R}_i \boldsymbol{R}_i^H \boldsymbol{q}_i^* \right] \tag{24}$$

Note that if the noise in the channels is temporally or spatially correlated, this is easily incorporated in Eq. (24). It is not necessary to know φ_o^2 to perform sensor location. From Eq. (21), it can be seen that $\boldsymbol{R}_i$ is a block diagonal matrix formed by $(\boldsymbol{G}_i = \boldsymbol{G}_{i0} - z_i \boldsymbol{G}_{i1})$. That is,

$$\boldsymbol{R}_i = \begin{bmatrix} \boldsymbol{G}_i & 0 & \cdots & 0 \\ 0 & \boldsymbol{G}_i & \cdots & 0 \\ \vdots & \vdots & \ddots & 0 \\ 0 & 0 & \cdots & \boldsymbol{G}_i \end{bmatrix} \tag{25}$$

Now, partition the right eigenvector matrix as $\boldsymbol{Q}=[\boldsymbol{Q}_1^T\ \boldsymbol{Q}_2^T\ \cdots\ \boldsymbol{Q}_s^T]^T$ and then partition $\boldsymbol{Q}_j$ as $\boldsymbol{Q}_j = [\boldsymbol{q}_{j1}\ \boldsymbol{q}_{j2}\ \cdots\ \boldsymbol{q}_{jm}]$. Then Eqs. (20) and (24) can be rewritten as the sum of small size matrices, i.e.,

$$\delta z_i = \sum_{j=1}^{s} \boldsymbol{q}_{ji}^T \boldsymbol{G}_i \varepsilon_j \tag{26}$$

$$\operatorname{var}(\delta z_i) = \sum_{j=1}^{s} \varphi_o^2 \left[\boldsymbol{q}_{ji}^T \boldsymbol{G}_i \boldsymbol{G}_i^H \boldsymbol{q}_{ji}^*\right]$$

$$= \sum_{j=1}^{s} \varphi_o^2 \left[\boldsymbol{q}_{ji}^T \boldsymbol{H}_i \boldsymbol{q}_{ji}^*\right] \tag{27}$$

where

$$\boldsymbol{H}_i = \boldsymbol{G}_i \boldsymbol{G}_i^H \tag{28}$$

Investigating the properties of matrix $\boldsymbol{H}_i$, it can be shown that $\boldsymbol{H}_i$ is Toeplitz and Hermitian where the diagonal terms are much larger than the off-diagonal terms. Equation (27) gives the variance of the ith frequency and damping values, which is a function of the sensor locations. The sensor placement technique is developed next, using the backward elimination method. The backward elimination method involves the removal of the least effective sensor, and this necessitates an efficient scheme for calculating the effect of each sensor on the variance. This effect is determined by examining the removal of each sensor and evaluating the resulting variance. Note that, although a brute-force approach of removing a location and recalculating the variance by Eq. (27) is possible, such a procedure ignores the abundance of information retained from one trial to the next and is therefore highly inefficient.

Perturbation Calculation

First, it is shown how to calculate $\Delta \boldsymbol{Q}^r$, which is the change of $\boldsymbol{Q}$ after deleting the rth output. The second part of this section then determines how the variances change after this process.

Let $\Delta \boldsymbol{V}_b$ be a deterministic perturbation of $\boldsymbol{V}_b$ [see Eq. (13)] introduced by deleting the rth output location:

$$\Delta \boldsymbol{V}_b^T = \begin{bmatrix} 0 & \cdots & 0 & \boldsymbol{V}_{br}^T & 0 & \cdots & 0 \end{bmatrix} \tag{29}$$

$$= \begin{bmatrix} 0 & \cdots & 0 & \boldsymbol{B}_r \boldsymbol{V}_k^T & 0 & \cdots & 0 \end{bmatrix} \tag{30}$$

Then,

$$\left[(\boldsymbol{V}_b - \Delta \boldsymbol{V}_b)^T\right]^{\dagger} \left(\boldsymbol{V}_b^* - \Delta \boldsymbol{V}_b^*\right) = \left[(\boldsymbol{V}_b - \Delta \boldsymbol{V}_b)^T (\boldsymbol{V}_b - \Delta \boldsymbol{V}_b)^*\right]^{-1} \tag{31}$$

and

$$\left[(\boldsymbol{V}_b - \Delta \boldsymbol{V}_b)^T\right]^{\dagger} \left(\boldsymbol{V}_b^* - \Delta \boldsymbol{V}_b^*\right) = \left(\boldsymbol{V}_b^T \boldsymbol{V}_b^* - \boldsymbol{V}_{br}^T \boldsymbol{V}_{br}^*\right)^{-1} \tag{32}$$

The inverse of $(\boldsymbol{V}_b^T \boldsymbol{V}_b^* - \boldsymbol{V}_{br}^T \boldsymbol{V}_{br}^*)$ can be cast in the following form[28] [denoting $\boldsymbol{W} = (\boldsymbol{V}_b^T \boldsymbol{V}_b^*)^{-1}$]:

$$\left(\boldsymbol{V}_b^T \boldsymbol{V}_b^* - \boldsymbol{V}_{br}^T \boldsymbol{V}_{br}^*\right)^{-1} = \boldsymbol{W} + \boldsymbol{W}\boldsymbol{V}_{br}^T \left[\boldsymbol{I}_k - \boldsymbol{V}_{br}^* \boldsymbol{W} \boldsymbol{V}_{br}^T\right]^{-1} \boldsymbol{V}_{br}^* \boldsymbol{W} \tag{33}$$

Let

$$\boldsymbol{E}^r = \boldsymbol{V}_{br}^T \left[\boldsymbol{I}_k - \boldsymbol{V}_{br}^* \boldsymbol{W} \boldsymbol{V}_{br}^T\right]^{-1} \boldsymbol{V}_{br}^* \boldsymbol{W} \tag{34}$$

$$= \boldsymbol{V}_{br}^T \left[\boldsymbol{I}_k - \boldsymbol{Q}_r \boldsymbol{V}_{br}^T\right]^{-1} \boldsymbol{Q}_r \tag{35}$$

$$= \boldsymbol{V}_{br}^T \left[\boldsymbol{I}_k + \boldsymbol{Q}_r \boldsymbol{V}_{br}^T + \left(\boldsymbol{Q}_r \boldsymbol{V}_{br}^T\right)^2 + \cdots\right] \boldsymbol{Q}_r \tag{36}$$

$$= \boldsymbol{V}_{br}^T \boldsymbol{Q}_r \left[\boldsymbol{I}_m + \boldsymbol{V}_{br}^T \boldsymbol{Q}_r + \left(\boldsymbol{V}_{br}^T \boldsymbol{Q}_r\right)^2 + \cdots\right] \tag{37}$$

Finally,

$$\boldsymbol{E}^r = \boldsymbol{V}_{br}^T \boldsymbol{Q}_r \left[\boldsymbol{I}_m - \boldsymbol{V}_{br}^T \boldsymbol{Q}_r\right]^{-1} \tag{38}$$

The effort in calculating $\boldsymbol{E}^r$ has been largely reduced in going from Eq. (35) to Eq. (37). This makes the derivation of $\Delta \boldsymbol{Q}^r$ easier to obtain. Equation (32) can be expressed as the following:

$$\boldsymbol{Q} + \Delta \boldsymbol{Q}^r = \left[(\boldsymbol{V}_b - \Delta \boldsymbol{V}_b)^T\right]^{\dagger} \tag{39}$$

$$= \left(\boldsymbol{V}_b^* - \Delta \boldsymbol{V}_b^*\right)[\boldsymbol{W} + \boldsymbol{W}\boldsymbol{E}^r] \tag{40}$$

$$= \boldsymbol{V}_b^* \boldsymbol{W} + \boldsymbol{V}_b^* \boldsymbol{W}\boldsymbol{E}^r - \Delta \boldsymbol{V}_b^* \boldsymbol{W} - \Delta \boldsymbol{V}_b^* \boldsymbol{W}\boldsymbol{E}^r \tag{41}$$

$$= \boldsymbol{Q} + \boldsymbol{Q}\boldsymbol{E}^r - \begin{bmatrix} 0 \\ \vdots \\ 0 \\ \boldsymbol{Q}_r \\ 0 \\ \vdots \\ 0 \end{bmatrix} - \begin{bmatrix} 0 \\ \vdots \\ 0 \\ \boldsymbol{Q}_r \boldsymbol{E}^r \\ 0 \\ \vdots \\ 0 \end{bmatrix} \tag{42}$$

$$= \boldsymbol{Q} + \begin{bmatrix} \boldsymbol{Q}_1 \boldsymbol{E}^r \\ \vdots \\ -\boldsymbol{Q}_r \\ \vdots \\ \boldsymbol{Q}_s \boldsymbol{E}^r \end{bmatrix} \tag{43}$$

Hence $\Delta \boldsymbol{Q}^r$ can be calculated easily based on the left eigenvectors of the system matrix before deleting the rth location and $\boldsymbol{E}^r$. This step is crucial because it avoids the need for doing

$$\sum_{i=n+1}^{s} i$$

eigenvalue problems for $\boldsymbol{S}$ in the sensor location process, where n is the final number of sensors.

Technique for Sensor Placement

The approach for sensor placement can be achieved by the following derivation. Express $\Delta \boldsymbol{Q}^r$ as block components:

$$\Delta \boldsymbol{Q}^r = \left[\left(\Delta \boldsymbol{Q}_1^r\right)^T \quad \left(\Delta \boldsymbol{Q}_2^r\right)^T \quad \cdots \quad \left(\Delta \boldsymbol{Q}_s^r\right)^T\right]^T \tag{44}$$

where if $j \neq r$, and letting $\boldsymbol{E}^r = [\boldsymbol{e}_1^r\ \boldsymbol{e}_2^r\ \cdots\ \boldsymbol{e}_m^r]$, the jth component of $\Delta \boldsymbol{Q}^r$ can be given as

$$\Delta \boldsymbol{Q}_j^r = \left[\Delta \boldsymbol{q}_{j1}^r \quad \Delta \boldsymbol{q}_{j2}^r \quad \cdots \quad \Delta \boldsymbol{q}_{jm}^r\right] \tag{45}$$

$$= \left[\boldsymbol{Q}_j \boldsymbol{e}_1^r \quad \boldsymbol{Q}_j \boldsymbol{e}_2^r \quad \cdots \quad \boldsymbol{Q}_j \boldsymbol{e}_m^r\right] \tag{46}$$

and if $j = r$, then $\Delta \boldsymbol{Q}_r^r = -\boldsymbol{Q}_r$. Let v_r be the total variance of parameters after deleting the rth location. Then,

$$v_r = \sum_{i=1}^{m} \sum_{j=1}^{s} \varphi_o^2 \left\{\left[\boldsymbol{q}_{ji}^T + \left(\Delta \boldsymbol{q}_{ji}^r\right)^T\right] \boldsymbol{H}_i \left[\boldsymbol{q}_{ji}^* + \left(\Delta \boldsymbol{q}_{ji}^r\right)^*\right]\right\} \tag{47}$$

$$v_r = \sum_{i=1}^{m} \sum_{j=1}^{s} \varphi_o^2 \left[\boldsymbol{q}_{ji}^T \boldsymbol{H}_i \boldsymbol{q}_{ji}^H\right] + \sum_{i=1}^{m} \sum_{j=1}^{s} \varphi_o^2 \left[\boldsymbol{q}_{ji}^T \boldsymbol{H}_i \left(\Delta \boldsymbol{q}_{ji}^r\right)^* + \left(\Delta \boldsymbol{q}_{ji}^r\right)^T \boldsymbol{H}_i \boldsymbol{q}_{ji}^* + \left(\Delta \boldsymbol{q}_{ji}^r\right)^T \boldsymbol{H}_i \left(\Delta \boldsymbol{q}_{ji}^r\right)^*\right] \tag{48}$$

$$= v + \Delta v_r \tag{49}$$

where Δv_r is the increase in the variance after deleting the rth location and v is the original total variance before deleting the rth location. We also can express Δv_r as

$$\Delta v_r = \sum_{i=1}^{m} \sum_{j=1, j\neq r}^{s} \varphi_o^2 \left[\left(\boldsymbol{e}_i^r\right)^T \boldsymbol{Q}_j^T \boldsymbol{H}_i \boldsymbol{q}_{ji}^* + \boldsymbol{q}_{ji}^T \boldsymbol{H}_i \boldsymbol{Q}_j^* \left(\boldsymbol{e}_i^r\right)^* + \left(\boldsymbol{e}_i^r\right)^T \boldsymbol{Q}_j^T \boldsymbol{H}_i \boldsymbol{Q}_j^* \left(\boldsymbol{e}_i^r\right)^*\right] - \sum_{i=1}^{m} \varphi_o^2 \left[\boldsymbol{q}_{ri}^T \boldsymbol{H}_i \boldsymbol{q}_{ri}^*\right] \tag{50}$$

When the number of sensors is large, the values of $\boldsymbol{e}_i^r$ in $\boldsymbol{E}^r$ are small, and the term $[(\boldsymbol{e}_i^r)^T \boldsymbol{Q}_j^T \boldsymbol{H}_i \boldsymbol{Q}_j^* (\boldsymbol{e}_i^r)^*]$ can be neglected. Because the first

and second terms of Δv_r are complex conjugate, and because $\boldsymbol{H}_i$ is diagonally dominant, Eq. (50) can be rewritten as

$$\Delta v_r \simeq \sum_{i=1}^{m} h_i \varphi_o^2 \left\{ -\boldsymbol{q}_{ri}^T \boldsymbol{q}_{ri}^* + \sum_{j=1, j\neq r}^{s} 2\,\mathrm{Re}\left[\left(\boldsymbol{e}_i^r\right)^T \boldsymbol{Q}_j^T \boldsymbol{q}_{ji}^* \right] \right\} \quad (51)$$

where h_i is the diagonal element of $\boldsymbol{H}_i$. Applying some manipulations to Eq. (51), a simpler form can be obtained as

$$\Delta v_r \simeq \varphi_o^2 \left(\sum_{j=1, j\neq r}^{s} \mathrm{Re}\left\{ \mathrm{tr}\left[2(\boldsymbol{E}^r)^T \boldsymbol{R}_j \bar{\boldsymbol{H}} \right] \right\} - \mathrm{tr}(\boldsymbol{R}_r \bar{\boldsymbol{H}}) \right) \quad (52)$$

$$\Delta v_r \simeq \varphi_o^2 \mathrm{Re}\left(\mathrm{tr}\left\{ \left[2(\boldsymbol{E}^r)^T \boldsymbol{R} - \boldsymbol{R}_r \right] \bar{\boldsymbol{H}} \right\} \right) \quad (53)$$

where

$$\bar{\boldsymbol{H}} = \mathrm{diag}[h_1 \;\; h_2 \;\; \cdots \;\; h_m], \qquad \boldsymbol{R}_j = \boldsymbol{Q}_j^T \boldsymbol{Q}_j^*, \qquad \boldsymbol{R} = \sum_{j=1, j\neq r}^{s} \boldsymbol{R}_j$$

Note that because only the trace of the matrices is required, the full matrix evaluations need not be performed. Repeating the process, a variance difference vector, $\Delta \boldsymbol{v}$, can be obtained and a decision can be made as to which location can be deleted for the smallest increase in the variance of the parameters:

$$\Delta \boldsymbol{v} = [\Delta v_1 \quad \Delta v_2 \quad \cdots \quad \Delta v_s] \quad (54)$$

III. Evaluation of Performance

Figure 1 shows the performance of the perturbation variance method compared with the Monte Carlo simulations for calculating

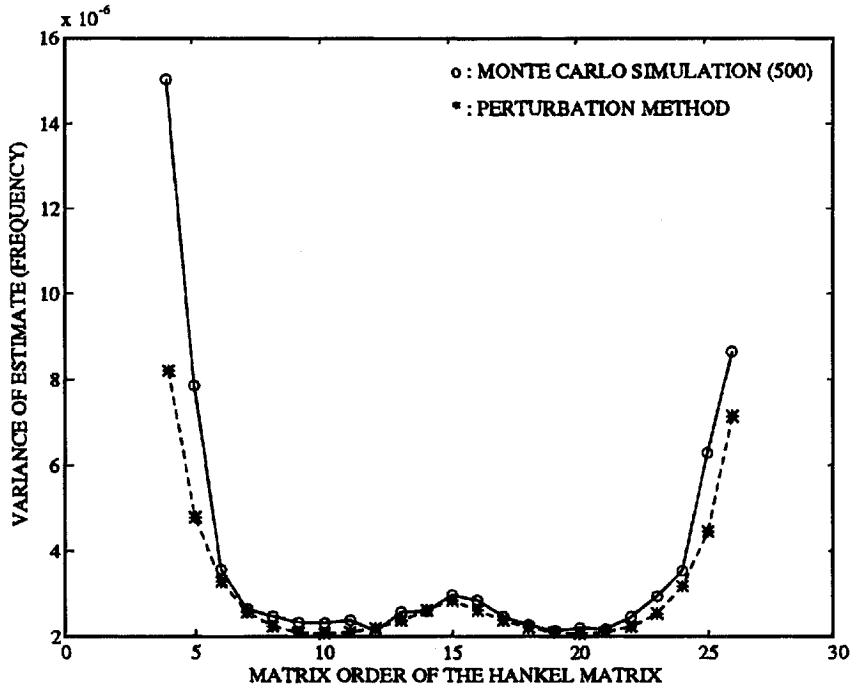

a) Mode 1

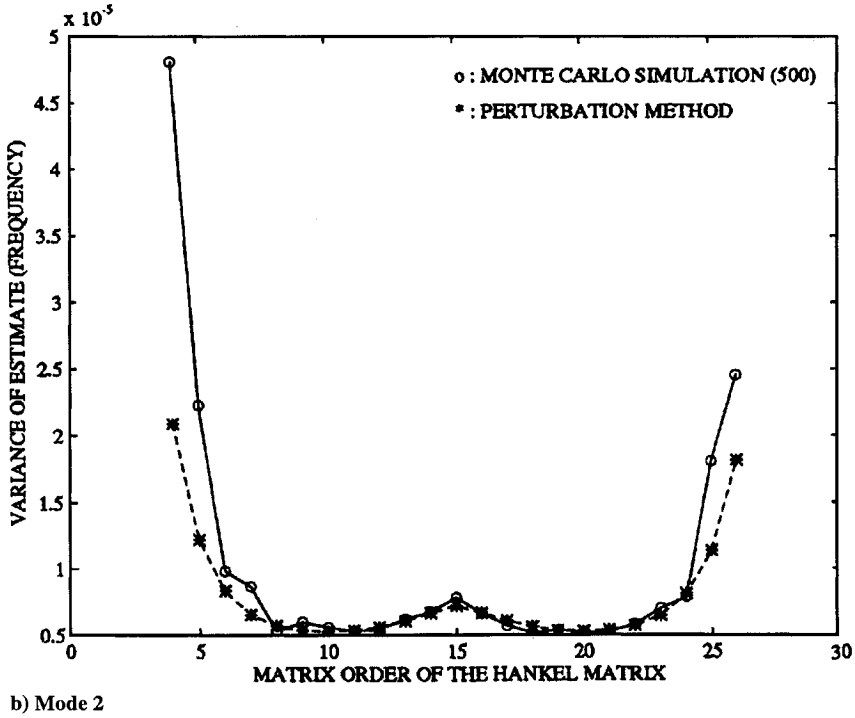

b) Mode 2

Fig. 1 Demonstration of the perturbation variance method.

Table 1 Frequencies and descriptions of nine truss target modes

Mode	Frequency, Hz	Description
7	124.98	First bending in y
8	125.08	First bending in x
9	173.53	First torsion in z
10	285.76	Second bending in y
11	286.80	Second bending in x
12	343.16	Second torsion in z
14	458.92	Third bending in y
15	463.37	Third bending in x
16	504.02	Third torsion in z

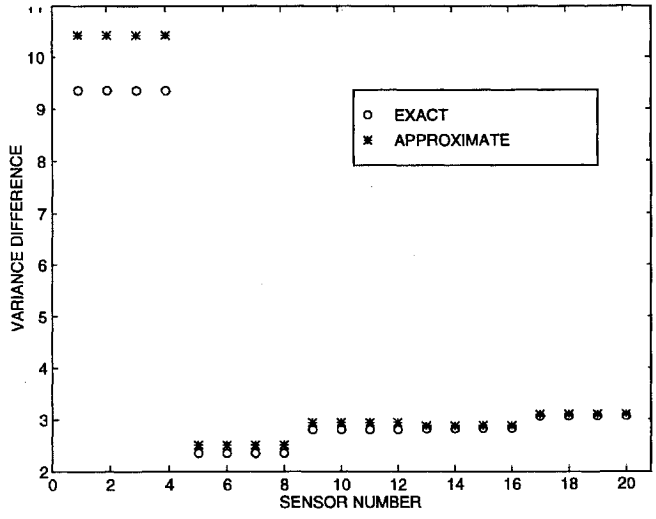

Fig. 2 Prediction of variance change on removing a sensor.

the variance of the estimated frequencies. It is a simple two-output two-mode case. The natural frequencies are [0.4 0.6] Hz, the damping factors are 0.1%, and the sampling frequency is 2 Hz. Results are for 500 different realizations of the data matrix with matrix orders from 4 to 26. The total number of samples was 30. These results indicate that a high level of accuracy can be achieved by the perturbation variance method with substantially fewer computations than with Monte Carlo simulations. The disadvantage of the Monte Carlo approach is the large computational cost that renders it impratical for sensor location.

Figure 2 shows the ability to predict the change in variances Δv, using the expression in Eq. (54), compared with the exact results [see Eq. (24)]. Note that the values are close to each other from these two methods, except for some of the larger variance differences. Because the location corresponding to the smallest Δv_i is removed in the sensor location process, the differences at large values of Δv_i would have little influence on the final results. In fact, it is not necessary to correctly predict each Δv_i; it is only necessary to preserve the relationship between the different values, thus ensuring that the sequence of retained sensors is unaltered. These results therefore show that the method expressed in Eq. (54) is very appropriate for sensor placement. It is also far more efficient than repeated use of Eq. (24).

The next examples demonstrate the effectiveness of the sensor placement method derived earlier. The results are compared with the effective independence (EfI) method[22–24] and the delta variance (DV) method.[25] In the end of this section, a result also is shown using the method of simulated annealing (SA).[29–31] The free-free structure is shown in Fig. 3. Nine fundamental main truss bending and torsion modes were selected as target modes for identification. Table 1 lists the natural frequencies and descriptions of the nine target modes. There are 44 nodes and a total of 132 degrees of freedom in the FEM of the structure. Selection of the initial candidate sensor set was based on the Euclidean norm of rows of the modal matrix. The norm for each row of modal matrix, which corresponds to each FEM physical degree of freedom, was

Table 2 Four frequency sets of modeling error

Mode	Frequency set, Hz			
	a	b	c	d
7	133.31	123.39	112.05	145.28
8	133.42	123.48	112.13	145.39
9	185.11	171.32	155.58	201.72
10	304.83	282.13	256.20	332.19
11	305.93	283.15	257.13	333.39
12	366.04	338.79	307.65	398.90
14	489.53	453.08	411.43	533.47
15	494.28	457.47	415.43	538.64
16	537.64	488.96	451.87	585.89

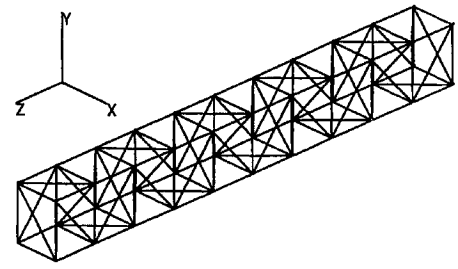

Fig. 3 Test article: 10-bay truss.

computed for the nine truss target modes. Degrees of freedom then were ranked according to their relative amplitude. The top 60 degrees of freedom were selected as the initial candidate set of sensor locations.

The sensor placement scheme depends on the properties of the data matrix given mainly by the total number of data samples and by the dimension of the Hankel matrices. In addition, this sensor placement procedure is a nonlinear experimental design technique and is therefore dependent on prior estimates of the unknown parameters. For comparison, a nominal truth model is assumed for which the damping values for all modes are 0.1%. It also is assumed that parameter estimation is performed using a time-domain method with Hankel matrices for each output of size 30×15 (i.e., $N = 45$, $k/h = \frac{1}{2}$). The sensor placement method was then applied to this nominal case to give nominal solutions for the sensor placement problem. These solutions are quantified in terms of the variance of estimates obtained with the nominal sensor locations.

To verify this sensor placement approach, the following cases have been studied using numerical simulations, and some observations have been gained in the sequel. Application of the tests results in different sensor locations, which may be considered as suboptimal for the nominal model. A comparison then is made between the variances obtained for the nominal sensor placement solution and those obtained from the following tests.

Effect of number of samples of each output (N). N is the length of each output that is used in constructing the Hankel matrices ($\boldsymbol{H}_0$ and $\boldsymbol{H}_1$). This test addresses the question of how much data is required for sensor placement. The final number of sensors to be kept is nine, which is the same as the number of target modes. In Eq. (11), it is known that h and k need to be kept larger than 18 and 2, respectively. That is, N has a value of at least 20.

Robustness to parameter uncertainty. 1) Damping effect test: A test seeking how the sensor placement results vary in terms of changes in the damping factors of the target modes. 2) Modeling error: Because of the difficulty of modeling a complex system, its properties (mass and stiffness distribution, etc.) are not precisely known. The original model is likely to contain parameter errors originating from assumptions about material characteristics, and mass distribution. These errors affect the frequency values and the mode shapes. Here, the material properties of the structure have been varied to represent modeling errors. Table 2 shows the changed frequencies of target modes.

Figures 4 and 5 are concerned with the effect of the number of response samples included in the estimation. It is shown that results for the deviation are all the same when $h \geq 18$ and $k \geq 3$. Hence, it

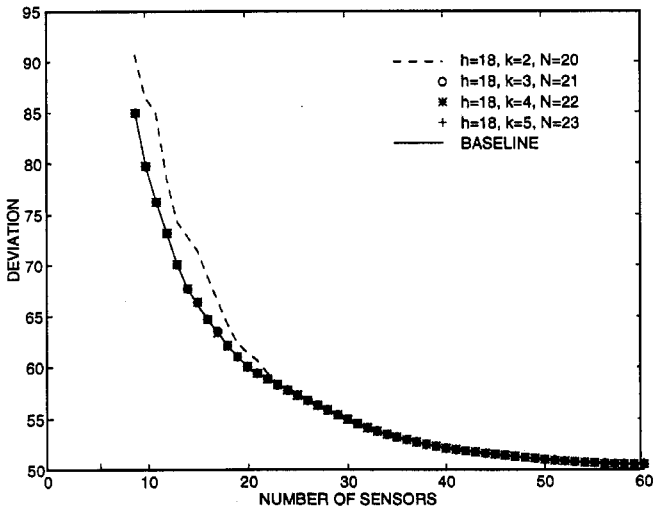

Fig. 4 Number of samples of each output (test 1).

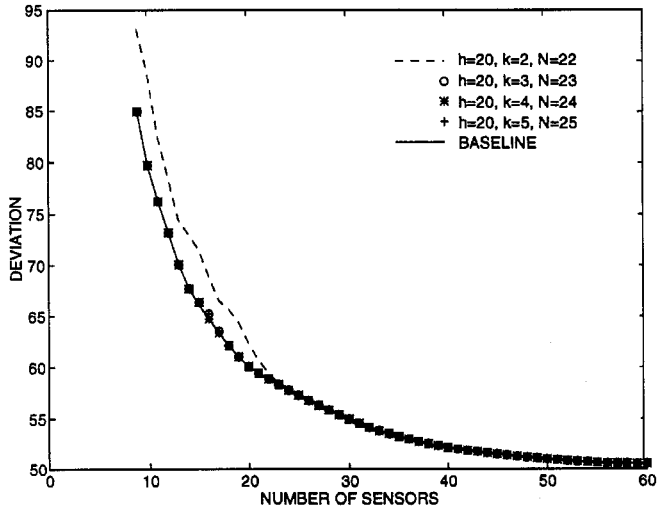

Fig. 5 Number of samples of each output (test 2).

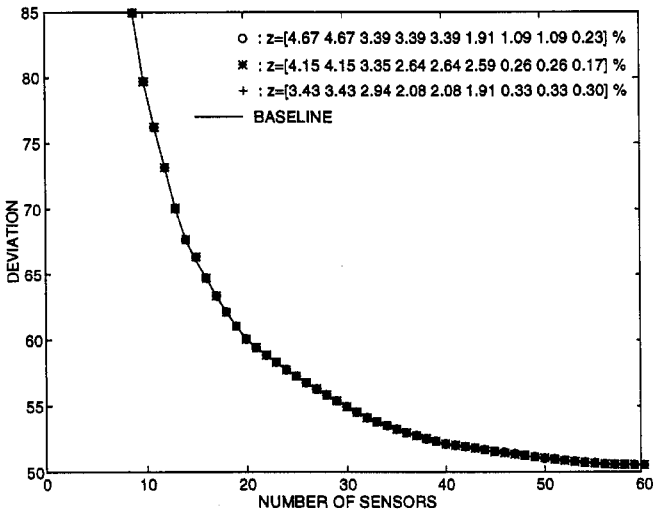

Fig. 6 Damping-effect test 1: damping values < 5%, $h = 18$, and $k = 3$.

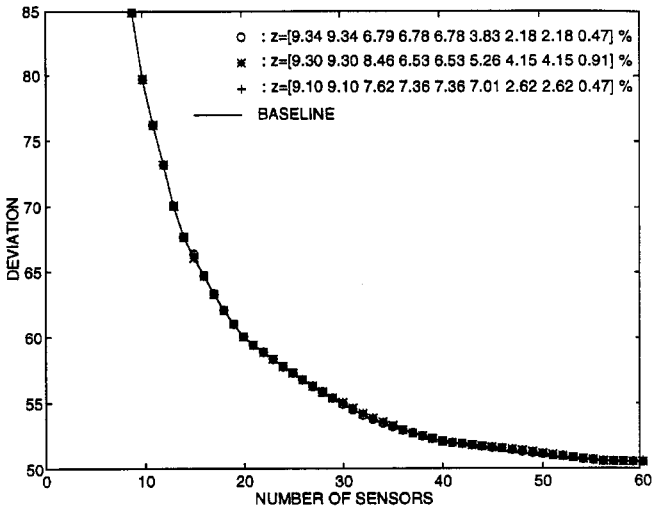

Fig. 7 Damping-effect test 2: damping values <10%, $h = 18$, and $k = 3$.

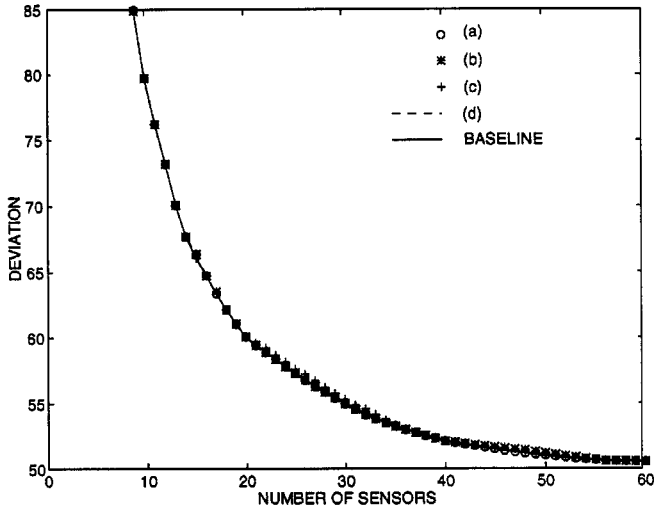

Fig. 8 Modeling-error test 1: damping values <5%, $h = 18$, and $k = 3$.

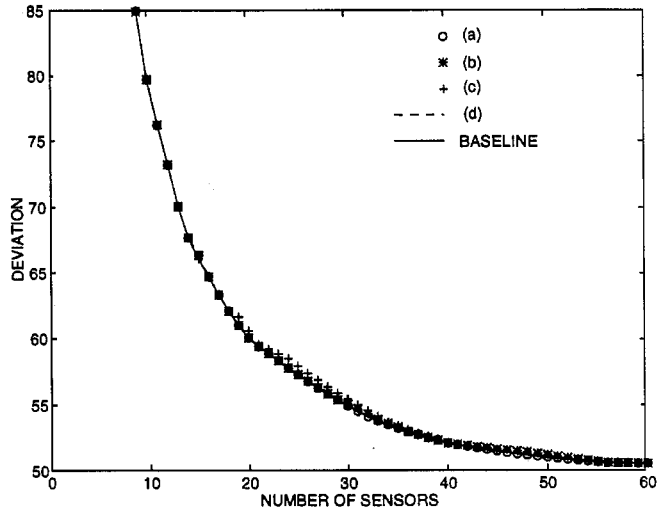

Fig. 9 Modeling-error test 2: damping values < 10%, $h = 18$, and $k = 3$.

can be determined that the threshold is $N = 21$ for steady ranking results. In Figs. 6 and 7, it can be seen that the sensor placement process is not affected by arbitrary variation of the damping values (<10%) of the target modes. This indicates that the approach for sensor placement is relatively independent of the value of damping factors of the parameters. In Figs. 8 and 9, the damping values of modes were varied arbitrarily, and the four cases of modeling error have been processed for sensor placement by the new approach. It is shown that the approach for sensor placement is robust to small modeling error.

In Fig. 10, the deviation of the estimates obtained from the variance-based, perturbation variance (PV) sensor location method is compared to those of the EfI and DV methods. These methods are also backward elimination methods except that they use different criteria based on modal responses. It could be seen that sensor location based on modal responses may not be best for modal parameter

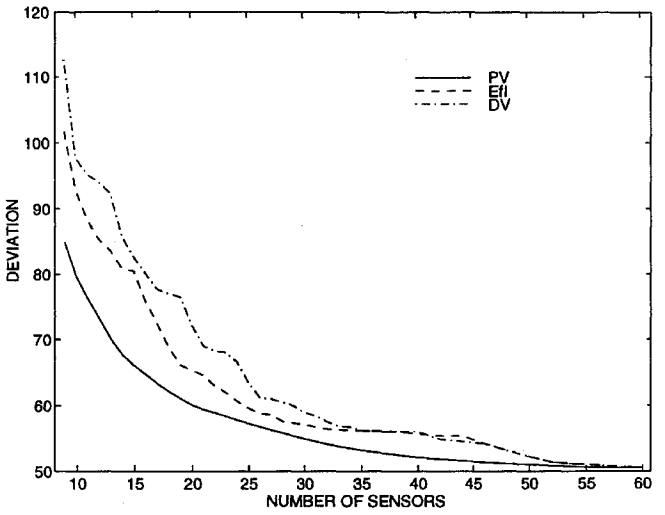

Fig. 10 Comparison of EfI, DV, and PV methods.

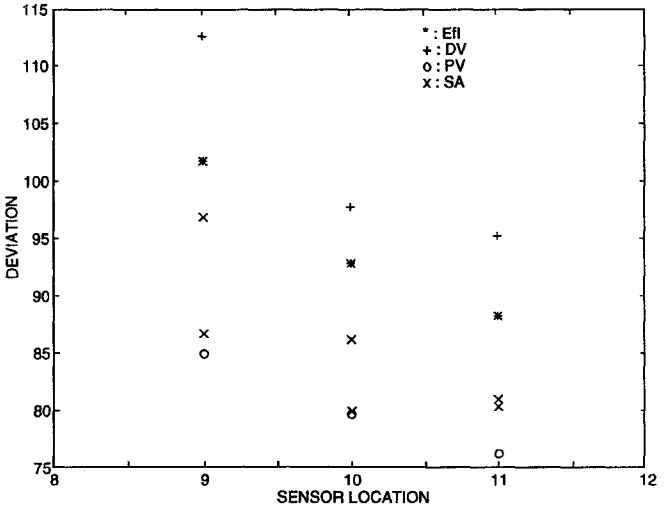

Fig. 11 Comparison of EfI, DV, PV, and SA with the sensor set of 9, 10, and 11.

identification. Finally, the results using an SA algorithm with the criteria given in Eq. (27) are compared with the other three methods. These results are shown in Fig. 11. In this case, the deviations of three final sets of sensors have been shown. The process of SA, being probabilistic, has been repeated several times.

Note that the deviation obtained from SA is not the smallest value among these comparisons. Although the deviation from SA has a high likelihood of hitting the global minimum, simulations obtained so far have failed to produce SA solutions better than the PV method, even for very slow cooling and the resulting long computation times. This situation is under further study because it may be problem dependent. In the limit for sufficiently slow cooling, the SA method would become an exhaustive search, which is extremely time-consuming. The preceding examples demonstrate the benefits of the new sensor placement method for modal parameter identification as well as its good properties with respect to modeling error. The excellent robustness may be explained in that the effect of small modeling errors would be to perturb the data matrices $\boldsymbol{H}_0$ and $\boldsymbol{H}_1$, which has some similarity to the effect of measurement noise on the estimation process. The overall sensor placement process may be viewed as picking sensor locations to minimize the effect of uncertainty in $\boldsymbol{H}_0$ and $\boldsymbol{H}_1$.

IV. Conclusion

This paper presents a special methodology for determining optimal sensor locations in dynamic systems that would enable the best identification of a given set of approximately known parameters of the system. The technique, based on the backward elimination scheme, utilizes the variance of estimates derived from a perturbation analysis of a time-domain method to determine the appropriate sensor locations. By examining the effect of the removal of a sensor, the recalculation of the perturbation variance has been largely simplified. To evaluate the robustness of this placement technique, modeling error was introduced to the FEM of the test structure by varying material properties. On the basis of the amount of material property variation, there was little effect seen on this sensor placement technique. The main advantage of this sensor placement method is that it is computationally nonintensive compared with the exhaustive search technique. The CPU times of the backward elimination method before and after applying simplification are 3 h and 5 min, respectively, for a problem of picking 10 sensors from 60. As with all backward elimination schemes, this method produces a ranking of the sensors. This perturbation variance method is very practical because it directly considers a time-domain estimator in solving the problem of sensor placement for modal parameter estimation. We have shown by comparison that the perturbation variance method is more efficient (i.e., smaller variance of estimates) than the EfI and DV methods for time-domain modal parameter estimation.

References

[1]Allemang, R. J., "Experimental Modal Analysis," *Modal Testing and Refinement*, ASME-59, American Society of Mechanical Engineers, New York, 1983, pp. 1–129.

[2]Ewins, D. J., *Modal Testing: Theory and Practice*, Research Studies Press, Wiley, New York, 1984, Chap. 4.

[3]Ibrahim, S. R., "Modal Confidence Factor in Vibrating Testing," *Journal of Spacecraft and Rockets*, Vol. 15, No. 5, 1978, pp. 313–316.

[4]Deblauwe, F., Brown, D. L., and Allemang, R. J., "The Polyreference Time Domain Technique," *5th International Modal Analysis Conference* Society for Experimental Mechanics, Bethel, CT, 1987, pp. 832–845.

[5]Leuridan, J. M., Brown, D. L., and Allemang, R. J., "Time Domain Parameter Identification Methods for Linear Modal Analysis: A Unifying Approach," *Journal of Vibration, Acoustics, Stress, and Reliability in Design*, Vol. 108, No. 1, 1986, pp. 1–8.

[6]Lembregts, F., and Snoeys, R., "Application and Evaluation of Multiple-Input Modal Parameter Estimation," *International Journal of Analytical and Experimental Modal Analysis*, Vol. 2, No. 1, 1987, pp. 19–31.

[7]Juang, J. N., and Pappa, R. S., "Effects of Noise on Modal Parameters Identified by the Eigensystem Realization Algorithm," *Journal of Guidance, Control, and Dynamics*, Vol. 9, No. 3, 1986, pp. 294–303.

[8]Juang, J. N., and Pappa, R. S., "An Eigensystem Realization Algorithm for Modal Parameter Identification and Modal Reduction," *Journal of Guidance, Control, and Dynamics*, Vol. 8, No. 5, 1985, pp. 620–627.

[9]Longman, R. W., and Juang, J. N., "A Variance Based Confidence Criterion for ERA Identified Modal Parameters," *Advances in Astronautical Sciences*, Vol. 65, No. 1, 1988, pp. 581–601.

[10]Longman, R. W., and Juang, J. N., "System Identification via Eigensystem Realization," *Journal of Guidance, Control, and Dynamics*, Vol. 12, No. 5, 1989, pp. 647–652.

[11]Fassois, S. D., Eman, K. F., and Wu, S. M., "A Linear Time Domain Method for Structural Dynamics Identification," *Journal of Vibration and Acoustics*, Vol. 112, No. 1, 1990, pp. 98–106.

[12]Hu, S., Chen, Y. B., and Wu, S. M., "Multi-Output Modal Parameter Identification by Vector Time Series Modeling," *Vibration Analysis—Techniques and Applications*, ASME DE-18-4, American Society of Mechanical Engineers, New York, 1989, pp. 259–265.

[13]Archibald, M., and Wicks, A. L., "An Alternative Time Domain System Identification Algorithm," *9th International Modal Analysis Conference*, Society for Experimental Mechanics, Bethel, CT, 1991, pp. 383–388.

[14]Mehta, N. P., and Pandit, S. M., "Modal Analysis of Multiple Eigenvalue Systems by Data Dependent Systems," *Journal of Vibration and Acoustics*, Vol. 113, No. 3, 1991, pp. 416–417.

[15]Pandit, S. M., and Mehta, N. P., "Data Dependent Systems Approach to Modal Analysis, Part 1: Theory," *Journal of Sound and Vibration*, Vol. 122, No. 3, 1988, pp. 413–432.

[16]Qureshi, Z. H., Ng, T. S., and Goodwin, G. C., "Optimum Experimental Design for Identification of Distributed Parameter Systems," *International Journal of Control*, Vol. 31, No. 1, 1980, pp. 21–29.

[17]Yu, T. K., and Seinfeld, J. H., "Observability and Optimal Measurement Location in Linear Distributed Parameter Systems," *International Journal of Control*, 1973, Vol. 18, No. 4, pp. 785–799.

[18]Omatu, S., Koide, S., and Soeda T., "Optimal Sensor Location Problem for a Linear Distributed Parameter System," *IEEE Transactions on Automatic Control*, Vol. AC-23, No. 4, 1978, pp. 665–673.

[19]Bayard, D. S., Hadaegh, F. Y., and Meldrum, D. R., "Optimal Experiment Design for Identification of Large Space Structures," 4th IFAC Symposium on the Control of Distributed Parameter Systems, Los Angeles, CA, June 1986.

[20]Delorenzo, M. L., "Sensor and Actuator Selection for Large Space Structure Control," *Journal of Guidance, Control, and Dynamics*, Vol. 13, No. 2, 1990, pp. 249–257.

[21]Miller, A. J., *Subset Selection in Regression*, Chapman and Hall, New York, 1990, pp. 51–53.

[22]Kammer, D. C., "Effects of Noise on Sensor Placement for On-Orbit Modal Identification of Large Space Structures," *Journal of Dynamic Systems, Measurement and Control*, Vol. 114, Sept. 1992, pp. 436–443.

[23]Kammer, D. C., "Sensor Placement for On-Orbit Modal Identification and Correlation of Large Space Structures," *Journal of Guidance, Control, and Dynamics*, Vol. 14, No. 2, 1991, pp. 251–259.

[24]Kammer, D. C., "Effect of Model Error on Sensor Placement for On-Orbit Modal Identification of Large Space Structures," *Journal of Guidance, Control, and Dynamics*, Vol. 15, No. 2, 1992, pp. 334–341.

[25]Hua, Y., and Sarkar, T. K., "Matrix Pencil Method for Estimating Parameters of Exponentially Damped/Undamped Sinusoids in Noise," *IEEE Transactions on Acoustics, Speech, and Signal Processing*, Vol. 38, No. 5, 1990, pp. 814–824.

[26]Wilkinson, J. H., *The Algebraic Eigenvalue Problem*, Oxford Univ. Press, Oxford, England, UK, 1988.

[27]Tasker, F. A., and Liu, C., "Effective Data Selection for Time Domain Modal Parameter Estimation," 11th IMAC Conf. (Kissimmee, FL), Feb. 1993.

[28]Campkell, S. L., and Meyer, C. D., Jr., *Generalized Inverses of Linear Transformations*, Dover, New York, Chap. 1.

[29]Corana, A., Marchesi, M., and Ridella, S., "Minimizing Multimodal Functions of Continuous Variables with the 'Simulated Annealing' Algorithm," *ACM Transactions on Mathematical Software*, Vol. 13, No. 3, 1987, pp. 262–280.

[30]Kirkpatrick, S., "Optimization by Simulated Annealing: Quantitative Studies," *Journal of Statistical Physics*, Vol. 34, Nos. 5/6, 1984, pp. 975–986.

[31]Kirkpatrick, S., Gelatt, C. D., and Vecchi, M. P., "Optimization by Simulation Annealing," *Science*, Vol. 220, May 1983, pp. 671–680.